Transverse-momentum spectra of strange particles produced in Pb + Pb collisions at $\sqrt{s_{NN}} = 2.76$ TeV in the chemical nonequilibrium model

Viktor Begun,[1,2] Wojciech Florkowski,[1,3] and Maciej Rybczynski[1]
[1]*Institute of Physics, Jan Kochanowski University, PL-25406 Kielce, Poland*
[2]*Bogolyubov Institute for Theoretical Physics, 03680 Kiev, Ukraine*
[3]*H. Niewodniczański Institute of Nuclear Physics, Polish Academy of Sciences, PL-31342 Kraków, Poland*
(Received 2 June 2014; revised manuscript received 11 September 2014; published 24 November 2014)

We analyze the transverse-momentum spectra of strange hadrons produced in Pb + Pb collisions at the collision energy $\sqrt{s_{\rm NN}} = 2.76$ TeV for different centrality bins. Our approach combines the concept of chemical nonequilibrium with the single-freeze-out scenario. The two ideas are realized in the framework of the Cracow model, whose thermodynamic parameters have been established in earlier studies of the ratios of hadron multiplicities. The geometric parameters of the model are obtained from the fit to the spectra of pions and kaons, only. Using these parameters, we obtain an excellent description of the spectra of protons and the K^0_S, $K^*(892)^0$, and $\phi(1020)$ mesons. A satisfactory description is obtained for the Λ, Ξ, and Ω hyperons.

DOI: 10.1103/PhysRevC.90.054912 PACS number(s): 25.75.Dw, 25.75.Ld

I. INTRODUCTION

Thermal and statistical models of hadron production [1–19] have become the standard tools to analyze mean multiplicities of the particles produced in heavy-ion collisions. They have explained successfully the BNL Alternating Gradient Synchrotron (AGS) [5–7], the CERN Super Proton Synchrotron (SPS) [8–14], and the BNL Relativistic Heavy Ion Collider (RHIC) [15–20] data on hadronic abundances. Supplemented by the proper definition of the spacetime geometry and hydrodynamic flow at freeze-out, the statistical models allow us to describe the transverse-momentum spectra and other soft-hadronic observables [17–21]. Nevertheless, the recent CERN Large Hadron Collider (LHC) data on heavy-ion collisions show that the predictions of two popular versions of the statistical model (the chemical equilibrium model and the strangeness nonequilibrium model) give too large values for the kaon-to-pion ratio, $(K^+ + K^-)/(\pi^+ + \pi^-)$, and especially, for the ratio of protons to pions $(p + \bar{p})/(\pi^+ + \pi^-)$ [22,23]. The recent fit [24] gives values for protons and antiprotons almost three standard deviations higher compared to the LHC data. The pions, kaons, and protons are the most abundant particles that are produced in heavy-ion collisions; therefore, this discrepancy is very uncomfortable for the thermal interpretation of hadron production. The problem with the correct description of protons is sometimes referred to as the *proton puzzle* [25].

Besides the problems with thermal interpretation of the hadron abundances at the LHC, one encounters also problems with the hydrodynamic interpretation of the transverse-momentum spectra of pions, kaons, and protons; see Fig. 1 in Ref. [22] and Figs. 13, 14, and 15 of Ref. [23]. The ratios of data and model analyzed in Ref. [23] have a very characteristic convex shape. Quite a few hydrodynamic models are discussed in Ref. [23]: Viscous Israel-Stewart 2+1 Hydrodynamics with UrQMD (VISH2 + 1) [26], Hydro-Kinetic Model (HKM) [27], Energy-sharing, Parton Multiple scattering with Outshell remnants and Screening model (EPOS) [28], and Krakow [29].[1] All these models exhibit a deficit in the very low-p_T region, with the largest effect of about 25–50% for pions in the most central collisions (c = 0–5%). In the ultraperipheral collisions (c = 70–80%), the models fail to reproduce the data at both the low and high transverse momenta. Similar features appear in the calculations presented in Refs. [30] and [31]. This situation is quite surprising, as the hydrodynamic models are supposed to work at low momenta, say, up to $p_T \sim 2$ GeV.

At least four concepts have been already introduced to explain the proton puzzle: the nonequilibrium hadronization, inelastic interactions in the hadronic phase, incomplete list of hadrons, and flavor hierarchy at freeze-out; see a recent review [32] and references therein. However, each of these concepts has its weak points and the puzzle is not solved yet. Here we discuss only the nonequilibrium hadronization model, because in our earlier work we have found [33] that one can connect the proton puzzle with the anomalous behavior of the pion p_T spectra and solve the two problems within the chemical nonequilibrium version of the Cracow single freeze-out model.

Encouraged by the success of our approach, in this paper we extend our study to all centrality classes and all measured hadrons including the recently measured strange mesons and baryons. Following the same procedure as in Ref. [33], we take the values of *thermodynamic* parameters from Ref. [34] and find the model *geometric* parameters from the fit to the pion and kaon spectra, only. In the next step, with the same parameters we determine the spectra of other hadrons. In this work we show that this strategy leads to an excellent description of the spectra of $p + \bar{p}$, K^0_S, $K^*(892)^0$, and $\phi(1020)$. A satisfactory description is also obtained for Λ, Ξ, and Ω.

The paper is organized as follows: In Sec. II we introduce our approach based on the Monte Carlo version of the Cracow

[1]We note that the Krakow hydrodynamic model cited in Ref. [23] is different from the Cracow freeze-out model used in our paper, although the former uses also the concept of single freeze-out at the end of the hydrodynamic evolution.

model as implemented in the THERMINATOR code [35,36]. The parameters of the model are fixed by the fits to the pion and kaon spectra, which are described in Sec. III. The results showing the p_T spectra of strange particles are presented in Sec. IV. The general discussion of our physics results in Sec. V and the two appendices close the paper.

II. THE CRACOW MODEL

A. The freeze-out spacetime geometry

The starting point for our considerations is the Cooper-Frye formula. The hadron rapidity and transverse-momentum distributions are calculated from the expression

$$\frac{dN}{dyd^2p_T} = E\frac{dN}{d^3p} = \int d\Sigma \cdot p\, f(p\cdot u), \tag{1}$$

where $d\Sigma_\mu = \tau_f\, r dr\, d\eta\, d\varphi\, u_\mu$ is an element of the freeze-out hypersurface and u^μ is the hydrodynamic Hubble-like flow at freeze-out:

$$u^\mu = \frac{x^\mu}{\tau_f} = \frac{(t,x,y,z)}{\tau_f}. \tag{2}$$

The parameter τ_f fixes invariant time at freeze-out, $\tau_f^2 = t^2 - x^2 - y^2 - z^2$. Hence, the freeze-out hypersurface may be conveniently parameterized with the help of three variables. In our case we use the transverse distance from the collision axis, $r = \sqrt{x^2+y^2}$, the spacetime rapidity, $\eta = 1/2\ln(t+z)/(t-z)$, and the azimuthal angle, $\varphi = \tan^{-1}(y/x)$. Since we consider a boost-invariant system, the integration over the spacetime rapidity η in Eq. (1) stretches from minus to plus infinity. On the other hand, the integration over r is restricted to the range $0 \leqslant r \leqslant r_{\max}$, where $r_{\max}$ defines the edge of a firecylinder. The quantities τ_f and $r_{\max}$ are the only two geometric parameters of the Cracow model.

The distribution function $f(pu)$ consists of primordial (directly produced) and secondary (produced by resonance decays) contributions. The decays are handled by THERMINATOR [35,36] and include all particles and well-established resonances. The primordial distribution of the ith hadron in the local rest frame has the form [37]

$$f_i(p,T,\Upsilon_i) = \frac{g_i}{\Upsilon_i^{-1}\exp\left(\sqrt{p^2+m_i^2}/T\right) \mp 1}. \tag{3}$$

Here g_i is the degeneracy factor connected with spin, m_i is the mass of the particle, Υ_i is the particle's fugacity, and T is the system's temperature. The -1 $(+1)$ sign corresponds to bosons (fermions).

The integration of the distribution function (3) over three-momentum gives the hadron density

$$n_i(T,\Upsilon_i) = \int \frac{d^3p}{(2\pi)^3}\, f_i(p,T,\Upsilon_i). \tag{4}$$

Similarly, the integration of the distribution (1) over transverse-momentum gives the rapidity distribution dN/dy. In Appendix A we show that the freeze-out geometry of our model implies the relation[2]

$$\frac{dN_i}{dy} = \frac{dN_i}{d\eta} = \pi r_{\max}^2 \tau_f\, n_i(T,\Upsilon_i). \tag{5}$$

Consequently, the knowledge of the thermodynamic parameters together with the rapidity density allows us to determine the system's volume per unit rapidity,

$$\frac{dV}{dy} = \pi r_{\max}^2 \tau_f. \tag{6}$$

As we shall see below, an independent experimental estimate of this quantity may serve us to reduce the number of independent geometric parameters of our model from two to just one.

B. Implementation of the chemical nonequilibrium

The difference between equilibrium and nonequilibrium models resides in the pre-exponential part of the fugacity factor Υ_i:

$$\Upsilon_i = \gamma_q^{N_q^i+N_{\bar q}^i}\gamma_s^{N_s^i+N_{\bar s}^i}\exp\left(\frac{\mu_Q Q_i + \mu_B B_i + \mu_S S_i}{T}\right), \tag{7}$$

where γ_q and γ_s are the nonequilibrium parameters, N_q^i and N_s^i are the numbers of light (u,d) and strange (s) quarks in the ith hadron, while $N_{\bar q}^i$ and $N_{\bar s}^i$ are the numbers of the antiquarks in the same hadron. The μ_Q, μ_B, and μ_S are the electric, baryon, and strange chemical potentials in the system, while Q_i, B_i, and S_i are the electric charge, baryon number, and strangeness of the ith hadron [33,37]. The chemical potentials are very small at the LHC energies. Therefore, for simplicity,[3] we set $\mu_Q = \mu_B = \mu_S = 0$ and obtain

$$\Upsilon_i = \gamma_q^{N_q^i+N_{\bar q}^i}\gamma_s^{N_s^i+N_{\bar s}^i}. \tag{8}$$

The term *nonequilibrium* comes from the fact that the case with $\gamma_q \neq 1$ and $\gamma_s \neq 1$ is equivalent to the introduction of the nonequilibrium chemical potentials $\mu_q/T = \ln\gamma_q$ and $\mu_s/T = \ln\gamma_s$ through the relation

$$\Upsilon_i \equiv \exp\left(\frac{\mu_q\left(N_q^i+N_{\bar q}^i\right)+\mu_s\left(N_s^i+N_{\bar s}^i\right)}{T}\right). \tag{9}$$

From Eq. (9) one can conclude, for example, that the conditions $\mu_i > 0$ or $\gamma_i > 1$ $(i = q,s)$ mean that the number of quark and antiquark pairs in this case is larger than the corresponding equilibrium number obtained with the same temperature. This kind of phenomenon may appear because of fast expansion and cooling of the strongly interacting system. It can be also a result of the interplay between annihilation and recombination

[2]We stress that η denotes the spacetime rapidity in our model; hence, Eq. (5) means that the *spacetime rapidity* distribution is equal to the *rapidity* distribution. On the other hand, the *pseudorapidity* and *rapidity* densities are usually quite different, especially at $y = 0$ [21].

[3]This assumption does not affect our results, because we do not consider very small differences between particles and antiparticles at the LHC and analyze only their total number. We also neglect the contributions from the charmed hadrons in Eqs. (7) and (8).

processes. For example, a $p\bar{p}$ annihilation to n pions would produce the relation between nucleon and pion chemical potentials[4]

$$2\mu_N = n\mu_\pi. \tag{10}$$

Generally, n may depend on energy; however, Eq. (8) postulates that $n = 3$. One can also imagine a QCD mechanism like the gluon condensation followed by the formation of low momentum $q\bar{q}$ pairs which fuse into pions, which subsequently condense [38]; see also [39,40].

Roughly speaking, one can say that in the nonequilibrium statistical model the extra degrees of freedom parametrize the effects connected with a departure from the equilibrium physics. However, using Eqs. (8) and (9) we imply that there are only two parameters responsible for deviations from the standard statistical model—for all particles the corrections scale in the way corresponding to their quark content. In this work, similarly to our previous paper [33], we compare two cases: the nonequilibrium statistical hadronization version of the Cracow model (NEQ SHM), where $\gamma_q \neq 1$ and $\gamma_s \neq 1$, and the equilibrium version (EQ SHM), where $\gamma_q = \gamma_s = 1$.

In typical calculations, the use of the parameter γ_s does not lead to substantial modifications of other thermodynamic parameters, like temperature or volume, but helps to describe strange particles. The appearance of γ_s can be explained, for example, in the so-called core-corona model [41–44], where a superposition of two sources of particle production is taken into account: single nucleon-nucleon (NN) collisions and a fully equilibrated source.

The use of $\gamma_q > 1$ (to our knowledge, introduced for the first time in Ref. [38]) makes the freeze-out temperature and/or volume smaller, because it influences the most abundant particles in the medium: Pions are multiplied by γ_q^2 while protons by γ_q^3. The temperature found in the recent chemical nonequilibrium calculations [34] is about 140 MeV. It is lower than the transition temperature obtained by the Wuppertal-Budapest Collaboration, $T_c = 150$–170 MeV. We note, however, that direct comparisons of the chemical nonequilibrium models (i.e., the models with $\gamma_s \neq 1$ and/or $\gamma_q \neq 1$) with the lattice simulations is inappropriate, since the lattice simulations are done for full chemical equilibrium. Furthermore, the temperature of freeze-out may be not connected with the phase transition temperature—we expect only that the latter is higher than the former.

We note that the value of γ_q used in Ref. [34] is equivalent to the pion chemical potential $\mu_\pi = 2T \ln \gamma_q \simeq 134$ MeV, which is very close to the π^0 mass, $m_{\pi^0} \simeq 134.98$. It may suggest that a substantial part of π^0 mesons form the condensate. Since the prediction of the Bose condensation in 1924 [45,46] the beauty and simplicity of this phenomenon have attracted the attention of many physicists [39,40,47–56]. However, only recently it has been confirmed experimentally in the system of cold atoms [57,58]. The high-temperature Bose condensation on the MeV $\sim 10^{12}$ K scale is also possible even in very small systems which are created in elementary particle collisions [59]. The Bose condensate formed in the ultrarelativistic regime has been considered in Refs. [60,61] as a dark-matter candidate in cosmological models. There are also interesting effects that appear inside of the pion condensate; see, e.g., Ref. [62]. Besides that, large pion chemical potentials may lead to the formation of other types of condensates like a diquark Bose condensate [63,64]. All those findings indicate at the importance of further studies of the Bose condensation phenomenon in high-energy physics.

[4]Using the Gibbs free energy one can show that the coefficients multiplying chemical potentials in equilibrium are equal to the coefficients appearing in the definition of the process. Equation (10) describes the equilibrium among protons, antiprotons, and pions *only*, with the condition that a $p\bar{p}$ pair produces exactly n pions. We thank Edward Shuryak for pointing out this relation to us.

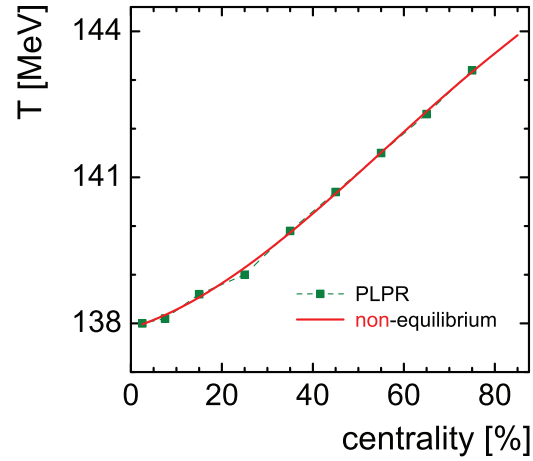

FIG. 1. (Color online) Temperature T shown as a function of centrality for the chemical nonequilibrium model (solid red [gray] line). The results from Ref. [34] are denoted as PLPR.

III. FIXING MODEL PARAMETERS—SPECTRA OF PIONS AND KAONS

As in our previous work [33], we use the thermodynamic parameters of the NEQ SHM model determined first in Ref. [34]. In Ref. [33] we used the values of T, γ_q, and γ_s from Ref. [34] and determined the values of $r_{\max}$ and τ_f from the χ^2 fit to the spectra of pions and kaons. In this work we adapt a simpler method—in addition to T, γ_q, and γ_s we use also the value of the volume dV/dy determined in Ref. [34]. The latter introduces a relation between $r_{\max}$ and τ_f; see Eq. (6). Hence, we need to fit only one parameter, which we choose to

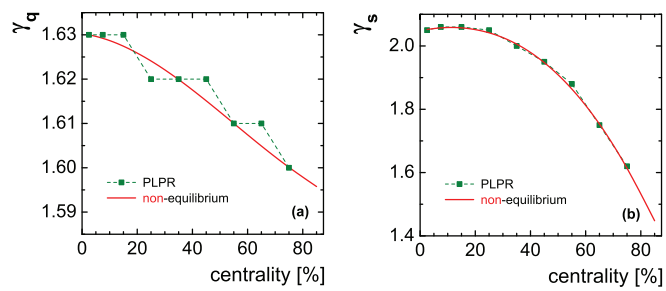

FIG. 2. (Color online) The parameters γ_q (a) and γ_s (b) as functions of centrality for the chemical nonequilibrium model.

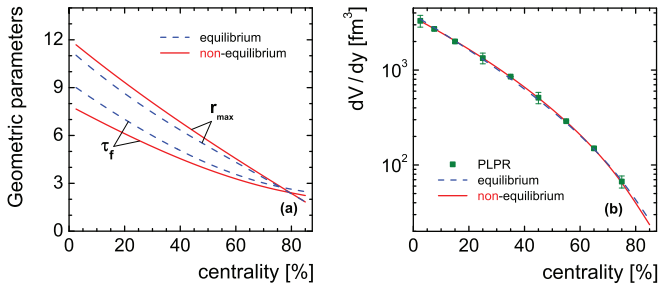

FIG. 3. (Color online) Geometric parameters (a) and the volume per unit rapidity (b) for both the chemical nonequilibrium and chemical equilibrium models.

be the ratio $r_{\max}/\tau_f$. In multiple calculations we have verified that the use of T, γ_q, and γ_s from Ref. [34] together with the two-dimensional fit of $r_{\max}$ and τ_f leads to the same results as the use of T, γ_q, γ_s, and dV/dy from Ref. [34] along with the one-dimensional fit of $r_{\max}/\tau_f$.

In order to analyze the centrality classes that are different from those studied in Ref. [34] and to facilitate the numerical manipulations, we use polynomial approximations for the functions $T(c)$, $\gamma_q(c)$, $\gamma_s(c)$, and $dV/dy(c)$. They are explicitly given in Appendix B. In practice, for the centrality class defined by the range $c = c_1$–c_2%, we use the values from the middle of the range; for example, we take $T((c_1 + c_2)/2)$. Having determined the optimal value of $r_{\max}/\tau_f$ for each studied centrality class, we use it to make predictions for the p_T spectra of protons and other hadron species.

In Fig. 1 we show the centrality dependence of the temperature T used in NEQ SHM. The small squares represent the values taken from Ref. [34], the dashed line (denoted as PLPR) is the interpolation of the results found in Ref. [34], and the red (gray) line represents our approximation. In Figs. 2(a) and 2(b), we show the two analogous plots of $\gamma_q(c)$ and $\gamma_s(c)$. In Fig. 3 we show the geometric parameters (a) and the volume per unit rapidity (b) for both the chemical nonequilibrium and chemical equilibrium models. In the EQ SHM version

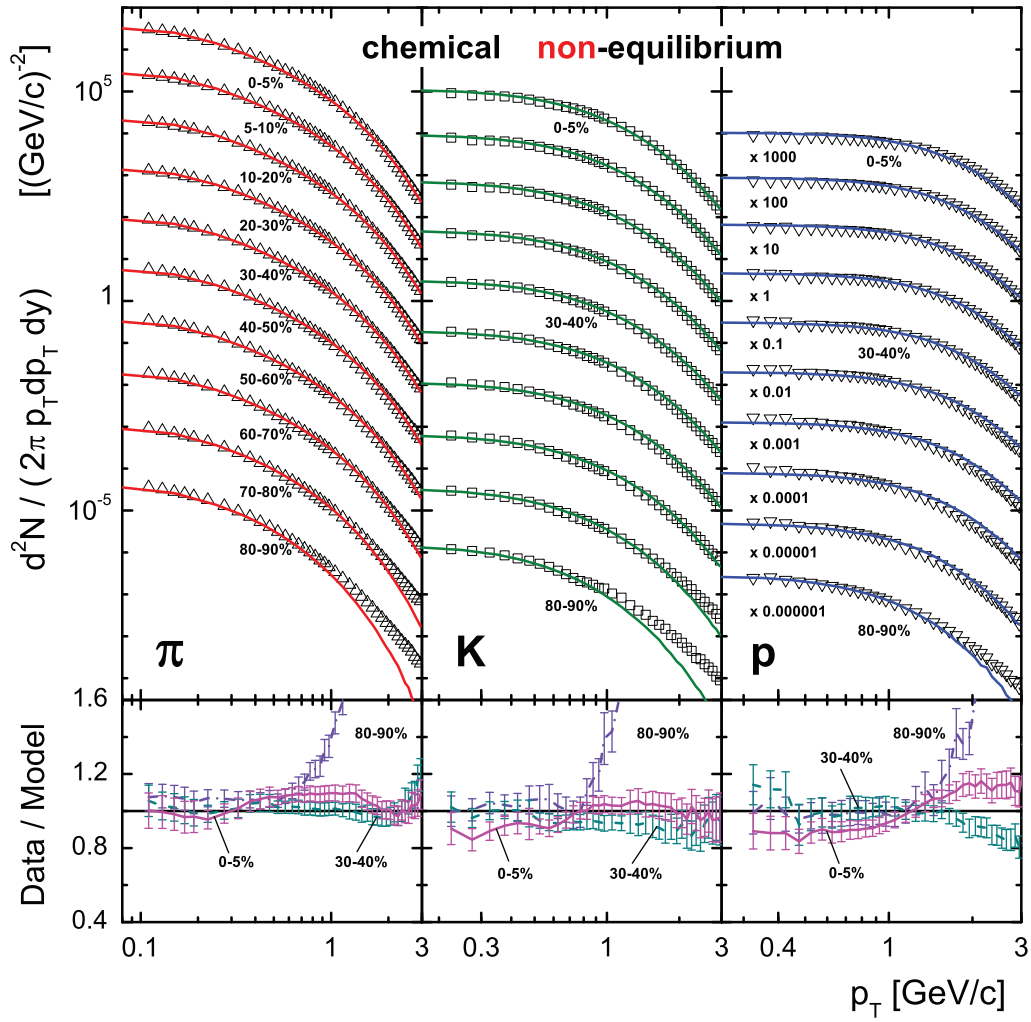

FIG. 4. (Color online) Upper panels: Transverse-momentum spectra of pions (left), kaons (middle), and protons (right) in different centrality classes. The data [23] are shown by the open symbols. The calculations in the nonequilibrium version of the Cracow model are indicated by the lines. Lower panels: The ratios of the experimental and theoretical p_T spectra in the most central ($c = 0$–5%), semiperipheral ($c = 30$–40%), and ultraperipheral ($c = 80$–90%) collisions for pions, kaons, and protons.

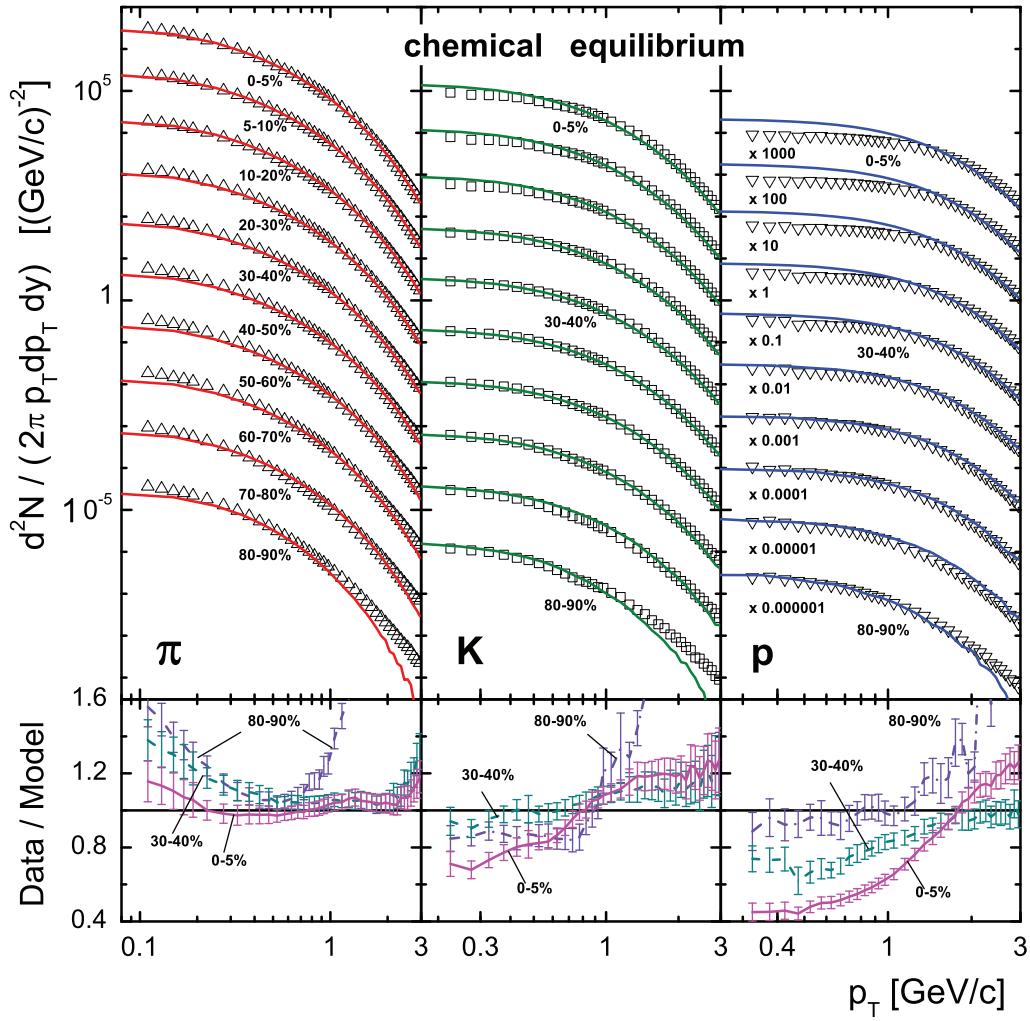

FIG. 5. (Color online) Same as Fig. 4 but in the equilibrium Cracow model.

we fix the temperature to be the same for all centralities, $T = 165.6$ MeV, and fit both $r_{\max}$ and τ_f. In this case, once again we fit first the pion and kaon spectra only and use the obtained parameters for all other particles. It is interesting to notice that although the geometric parameters are different for NEQ SHM and EQ SHM the volume per unit rapidity remains almost unchanged if we fix the centrality class.

The results of our calculations for pions, $\pi^+ + \pi^-$, kaons, $K^+ + K^-$, and protons, $p + \bar{p}$, are shown in Fig. 4 for NEQ SHM and in Fig. 5 for EQ SHM. We consider all centralities and the whole p_T range provided by the experiment for pions and kaons. In order to show all centralities together we have multiplied each spectrum at a given centrality by the factor displayed in the upper right panel. Experimental error bars in the upper panels are of the size of the symbols and, therefore, they are not shown. The logarithmic scale used for the p_T axis emphasizes the low-p_T region. The lower panels show the data-to-model ratios for the most central, $c = 0$–5%, semiperipheral, $c = 30$–40%, and ultraperipheral collisions, $c = 80$–90%.

In the upper panels of Figs. 4 and 5 one can observe a good agreement for pions and kaons both for NEQ and EQ versions of the Cracow model in the wide p_T range and for all centralities. This agreement is a strong argument in favor of the parametrization (2) of the flow at freeze-out. On the other hand, the protons in central collisions are described only in NEQ, as we first observed in Ref. [33].

The agreement between the data and the model predictions is more clearly displayed in the lower panels of Figs. 4 and 5 where the linear vertical scale is used. The NEQ lines in the Cracow model go exactly through the experimental points for pions and kaons, for most central and semiperipheral collisions in the whole range from the lowest available point up to $p_T = 3$ GeV. The deviations appear only in ultraperipheral collisions for $p_T \gtrsim 1.5$ GeV. In spite of the fact that we fitted only pions and kaons, the agreement for protons is also very good.

Comparing Figs. 4 and 5 one can check that the NEQ fit is much better than the EQ fit. Moreover, in EQ SHM the demand of the best fit for pions and kaons bends pions up and kaons down at low p_T. The proton spectra behave similarly to the kaon spectra. The protons are so much in anticorrelation with the pions that a simultaneous fit of the low p_T part of the spectrum of pions and protons in EQ SHM seems to be impossible.

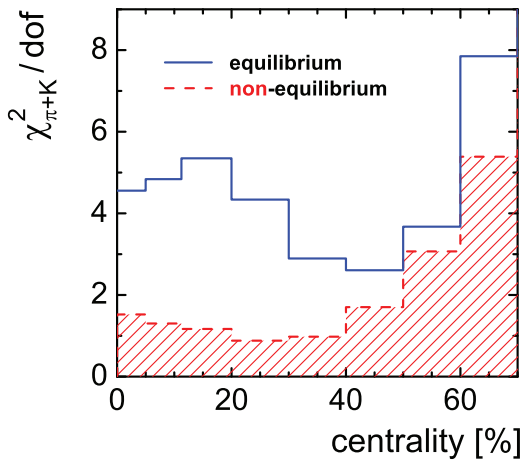

FIG. 6. (Color online) The centrality dependance of the χ^2 calculated for the joint fit of the p_T spectra of pions and kaons.

The quality of the fit in NEQ and EQ is illustrated in Fig. 6. The values of χ^2 indicate that NEQ SHM is three times better for central and semicentral collisions. Starting with the centrality of about 40%, the difference between NEQ and EQ SHM decreases while the values of χ^2 grow very rapidly. This behavior may be explained by the qualitative change of the spectra which are exponential in central and semicentral collisions and become well described by a power law in peripheral collisions.

IV. SPECTRA OF STRANGE PARTICLES

Another challenging test for the NEQ SHM model is a comparison of the model predictions with the data available for the p_T spectra of strange particles. In order to verify the model we use the same parameters as those found in the study of pions and kaons. We do not present here the results for the chemical equilibrium version, since it always yields much worse agreement with the data as compared to the chemical nonequilibrium version.

In the model analysis of the spectra of strange particles it is very important to take into account the same weak decay corrections as those considered by the experiment. The ALICE Collaboration does not specify the weak corrections for K^0_S; hence, we take into account the K^0_S's coming from all possible decays. The spectra of the Λ hyperons were corrected for the feed-down contributions coming from the weak decays of Ξ^- and Ξ^0. Therefore, we subtract the feed-down from these particles only. ALICE also did not correct the Λ spectra for the feed-down from nonweak decays of Σ^0 and from the $\Sigma(1385)$ family. All Σ^0 and 88.25% of $\Sigma^-(1385)$, $\Sigma^0(1385)$, and $\Sigma^+(1385)$ decay into Λ and are included in the Λ yield in THERMINATOR by default. The Ξ's and Ω's are directly taken from the generated events.

The results for K^0_S, $K^*(892)^0$, and $\phi(1020)$ are shown in Fig. 7. The error bars are indicated only if they are bigger than the corresponding symbols in the figure. One can see that the p_T spectra of these particles are fitted very well. For many centralities the NEQ model lines go through the experimental points. We stress that it is very nontrivial that the fit done initially for $\pi^+ + \pi^-$ and $K^+ + K^-$ only appears so good also for $p + \bar{p}$, K^0_S, $K^*(892)^0$, and $\phi(1020)$. These particles have a different quark content and therefore different nonequilibrium corrections according to Eq. (8). Moreover, the $K^*(892)^0$, in contrast to other particles, is a short-living resonance that could not interact frequently with the hadronic matter possibly formed in the final state. The fact that we fit its spectrum together with the long-living $\phi(1020)$ supports our picture of the nonequilibrium hadronization and the single freeze-out.

The model and experimental p_T spectra of the hyperons (Λ, $\Xi = \Xi^+ + \Xi^-$, and $\Omega = \Omega^+ + \Omega^-$) are shown in Fig. 8. One can see that the behavior of Λ is different from the behavior

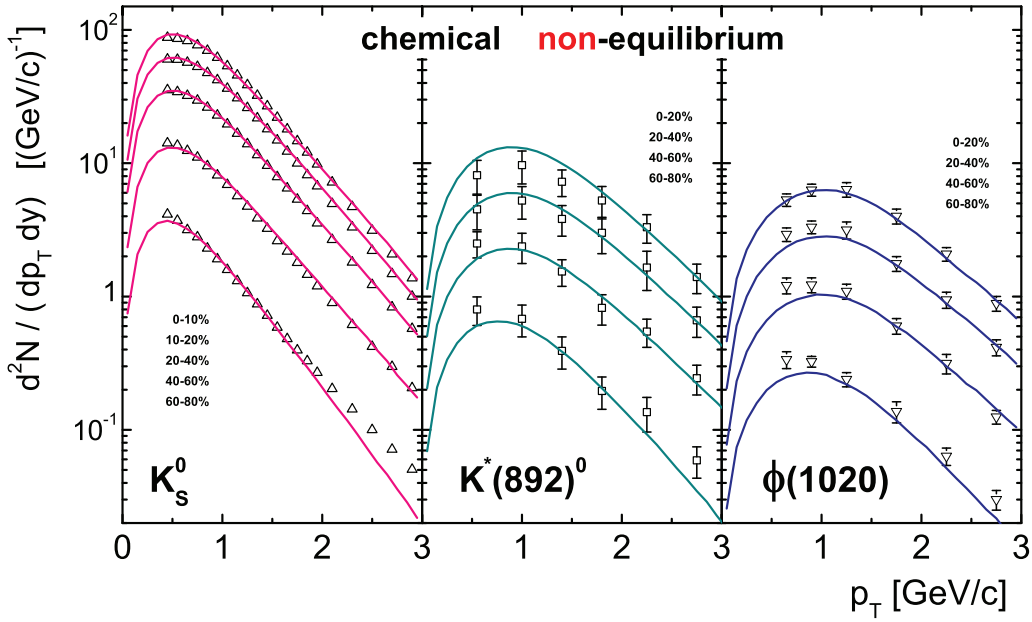

FIG. 7. (Color online) Transverse-momentum spectra of K^0_S (left), $K^*(892)^0$ (middle), and $\phi(1020)$ (right) in different centrality classes. The data [65,66] are shown by the open symbols. The calculations in the nonequilibrium Cracow model are indicated by the lines.

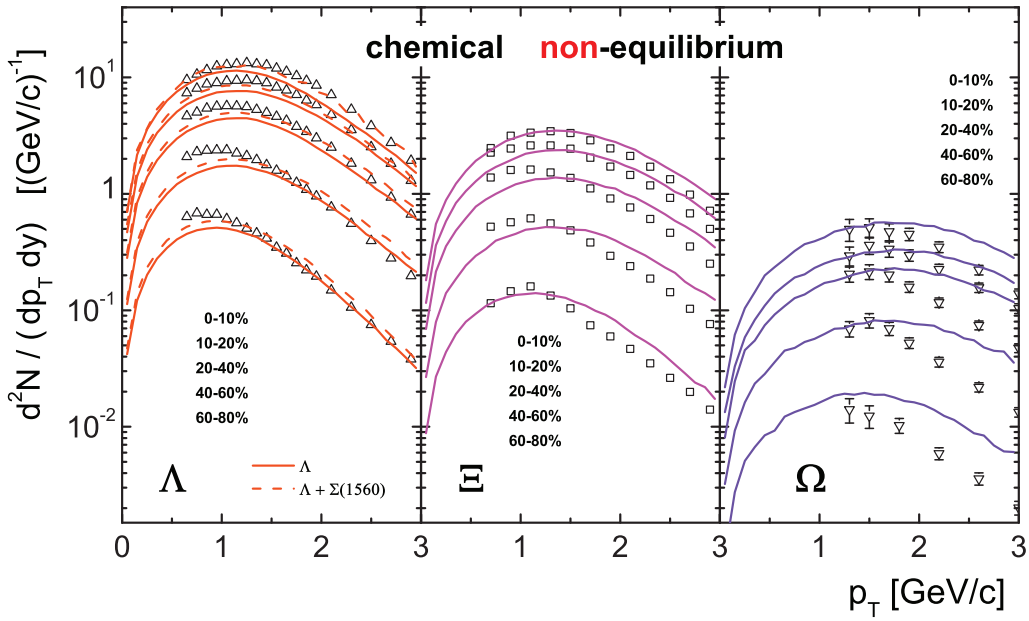

FIG. 8. (Color online) The same as in Fig. 7 but for Λ [65], Ξ, and Ω [67].

of Ξ and Ω. The typical shape of the Λ spectrum is similar to that observed in the data, but the overall normalization of the model spectrum is smaller. The experimental results for Ξ and Ω at low p_T are well reproduced, but for higher values of p_T ($p_T > 2$ GeV) the NEQ SHM model overshoots the data. One of the possible sources of these discrepancies may be the use of the thermodynamic parameters established earlier in Ref. [34]. At the time when Ref. [34] was written, the data on multistrange particles were not available. Therefore, the authors of Ref. [34] made an estimate of the yields of Λ, Ξ, and Ω. In a more recent paper they report lower values of γ_s and propose to take into account the Σ(1560) resonance that decays into Λ [68]. Unfortunately, the fit is done only for the c =10–20% centrality bin (this is so probably because ALICE made different centrality selections for different particles, and they coincide only for the c = 10–20% bin).

As we are mainly interested in the spectra, in this paper we do not refit the whole presently available set of data on mean multiplicities. Nevertheless, we can make an estimate of the effect of inclusion of the Σ(1560) decays into Λ in the similar way as it has been done in [68]. The result is shown in Fig. 8 by the dashed line. One can see that the agreement is improved with Σ(1560) included, especially for more central events. On the other hand, the peripheral events for Λ start to deviate from the data in a similar way as the calculations for Ξ and Ω. There is approximately the same area under the data and simulation curves, but we have too few particles at low p_T and too many at high p_T. This may be an artifact of the Cracow model that assumes a simple Hubble form of flow at freeze-out for all particles at all centralities; see Eq. (2). Thus, the excess at high p_T may be an indication that heavy particles in our model experience too much flow.[5]

[5]A similar conclusion was drawn from the blast wave fits presented in Ref. [69].

V. CONCLUSIONS

In this work we have analyzed the transverse-momentum spectra of strange hadrons produced in Pb + Pb collisions at the collision energy $\sqrt{s_{\rm NN}} = 2.76$ TeV. In this way, we have extended our approach initiated in Ref. [33], where we studied pions, kaons, and protons only. An additional new aspect of the present work is the complete analysis of the data collected at different centrality classes.

Our approach combines the concept of chemical nonequilibrium with the single-freeze-out scenario. To calculate the transverse-momentum spectra we have used the framework of the Cracow model with thermodynamic parameters established in earlier studies of the ratios of hadron abundances. The geometric parameters of the model have been obtained from the fit to the pion and kaon spectra. Using the same thermodynamic and geometric parameters, we have obtained an excellent description of the spectra of K^0_S's, $K^*(892)^0$'s, and $\phi(1020)$'s. These particles have different lifetimes, and the presence of a long hadronic phase after the chemical freeze-out would change the temperature parameters characterizing $K^*(892)^0$'s and $\phi(1020)$'s. Therefore, our simultaneous description of $K^*(892)^0$'s and $\phi(1020)$'s confirms the validity of the single-freeze-out approximation. A satisfactory description is also obtained for Λ, Ξ, and Ω.

Our general conclusion is that the chemical nonequilibrium model with essentially one extra geometric parameter allows for a good description of the spectra of all hadrons measured in heavy-ion collisions at the LHC energies. Since at lower energies the spectra were very well described by the equilibrium model with $\gamma_q = 1$ [70], it may suggest a new physics mechanism of particle production at the LHC.

ACKNOWLEDGMENTS

We thank Piotr Bozek, Jinfeng Liao, Christina Markert, Larry McLerran, Tigran Kalaydzhyan, and Edward Shuryak

TABLE I. Coefficients used in Eq. (B1) describing the centrality dependence of the thermodynamic and geometric parameters for the two versions of the model.

	Nonequilibrium					Equilibrium	
	$r_{\max}$	τ_f	T	γ_q	γ_s	$r_{\max}$	τ_f
A	12.046	7.89	137.91	1.63	2.05	11.42	9.31
B	-1.44×10^{-1}	-9.34×10^{-2}	2.57×10^{-2}	-6.17×10^{-5}	2.05×10^{-3}	-1.57×10^{-1}	-1.22×10^{-1}
C	3.97×10^{-4}	1.65×10^{-4}	1.08×10^{-3}	-8.34×10^{-6}	-7.69×10^{-5}	9.47×10^{-4}	2.90×10^{-4}
D	-1.40×10^{-6}	1.77×10^{-6}	-6.42×10^{-6}	5.05×10^{-8}	-3.56×10^{-7}	-4.98×10^{-6}	2.36×10^{-6}

for clarifying discussions and interesting comments. V.B and W.F. were supported by Polish National Science Center Grant No. DEC-2012/06/A/ST2/00390. M.R. was supported in part by Polish National Science Center Grant No. DEC-2011/01/D/ST2/00772.

APPENDIX A: RAPIDITY AND SPACETIME RAPIDITY DISTRIBUTIONS

Using our definition of the element of the freeze-out hypersurface $d\Sigma_\mu$ in Eq. (1) we may write

$$E\frac{dN}{d^3p} = \tau_f \int_0^{r_{\max}} r\,dr \int_{-\infty}^{+\infty} d\eta \int_0^{2\pi} d\varphi\, puf(pu). \quad \text{(A1)}$$

Integrating this equation over momentum gives

$$\frac{dN}{d\eta} = \tau_f \int_0^{r_{\max}} r\,dr \int_0^{2\pi} d\varphi\, u_\mu \int \frac{d^3p}{E}\, p^\mu f(pu). \quad \text{(A2)}$$

The covariant form of the last integral on the right-hand side in Eq. (A2) implies

$$\frac{dN}{d\eta} = \tau_f \int_0^{r_{\max}} r\,dr \int_0^{2\pi} d\varphi\, n(T,\Upsilon). \quad \text{(A3)}$$

If the freeze-out conditions correspond to constant values of T and Υ, the last factor in Eq. (A3) factorizes and we obtain the desired formula

$$\frac{dN}{d\eta} = \pi r_{\max}^2 \tau_f\, n(T,\Upsilon). \quad \text{(A4)}$$

In addition, the boost invariance of Eq. (A1) implies that the density $dN/d\eta$ is obtained from the expression whose general form may be written as

$$\frac{dN}{d\eta} = \int dy \int d^2p_T F(p_T, y-\eta), \quad \text{(A5)}$$

where F is a function of the difference $y-\eta$. From Eq. (A5) we conclude that

$$\frac{dN}{d\eta} = \frac{dN}{dy}. \quad \text{(A6)}$$

APPENDIX B: THERMODYNAMIC PARAMETERS AS FUNCTIONS OF CENTRALITY

In this section we present our approximate formulas for the centrality dependence of the thermodynamic and geometric parameters in the chemical nonequilibrium and chemical equilibrium models. All functions are approximated by the third-order polynomial of the form

$$A + Bc + Cc^2 + Dc^3, \quad \text{(B1)}$$

where c is given in percentages multiplied by 100. The appropriate coefficients are given in Table I.

[1] P. Koch and J. Rafelski, South Afr. J. Phys. **9**, 8 (1986).
[2] J. Cleymans and H. Satz, Z. Phys. C **57**, 135 (1993).
[3] J. Cleymans and K. Redlich, Phys. Rev. Lett. **81**, 5284 (1998).
[4] M. Gazdzicki and M. I. Gorenstein, Acta Phys. Polon. B **30**, 2705 (1999).
[5] P. Braun-Munzinger, J. Stachel, J. P. Wessels, and N. Xu, Phys. Lett. B **344**, 43 (1995).
[6] J. Cleymans, D. Elliott, H. Satz, and R. L. Thews, Z. Phys. C **74**, 319 (1997).
[7] F. Becattini, J. Cleymans, A. Keranen, E. Suhonen, and K. Redlich, Phys. Rev. C **64**, 024901 (2001).
[8] J. Sollfrank, M. Gazdzicki, U. W. Heinz, and J. Rafelski, Z. Phys. C **61**, 659 (1994).
[9] E. Schnedermann, J. Sollfrank, and U. W. Heinz, Phys. Rev. C **48**, 2462 (1993).
[10] P. Braun-Munzinger, J. Stachel, J. P. Wessels, and N. Xu, Phys. Lett. B **365**, 1 (1996).
[11] F. Becattini, J. Phys. G **23**, 1933 (1997).
[12] G. D. Yen and M. I. Gorenstein, Phys. Rev. C **59**, 2788 (1999).
[13] P. Braun-Munzinger, I. Heppe, and J. Stachel, Phys. Lett. B **465**, 15 (1999).
[14] F. Becattini, M. Gazdzicki, A. Keranen, J. Manninen, and R. Stock, Phys. Rev. C **69**, 024905 (2004).
[15] P. Braun-Munzinger, D. Magestro, K. Redlich, and J. Stachel, Phys. Lett. B **518**, 41 (2001).
[16] W. Florkowski, W. Broniowski, and M. Michalec, Acta Phys. Polon. B **33**, 761 (2002).
[17] W. Broniowski and W. Florkowski, Phys. Rev. Lett. **87**, 272302 (2001).
[18] W. Broniowski and W. Florkowski, Phys. Rev. C **65**, 064905 (2002).

[19] F. Retiere and M. A. Lisa, Phys. Rev. C **70**, 044907 (2004).
[20] W. Broniowski, A. Baran, and W. Florkowski, AIP Conf. Proc. **660**, 185 (2003).
[21] W. Florkowski, *Phenomenology of Ultrarelativistic Heavy-Ion Collisions* (World Scientific, Singapore, 2010).
[22] B. Abelev *et al.* (ALICE Collaboration), Phys. Rev. Lett. **109**, 252301 (2012).
[23] B. Abelev *et al.* (ALICE Collaboration), Phys. Rev. C **88**, 044910 (2013).
[24] J. Stachel, A. Andronic, P. Braun-Munzinger, and K. Redlich, J. Phys. Conf. Ser. **509**, 012019 (2014).
[25] M. Rybczynski, W. Florkowski, and W. Broniowski, Phys. Rev. C **85**, 054907 (2012).
[26] H. Song, S. A. Bass, and U. Heinz, Phys. Rev. C **89**, 034919 (2014).
[27] I. A. Karpenko, Y. M. Sinyukov, and K. Werner, Phys. Rev. C **87**, 024914 (2013).
[28] K. Werner, I. Karpenko, M. Bleicher, T. Pierog, and S. Porteboeuf-Houssais, Phys. Rev. C **85**, 064907 (2012).
[29] P. Bozek and I. Wyskiel-Piekarska, Phys. Rev. C **85**, 064915 (2012).
[30] L. Pang, Q. Wang, and X.-N. Wang, Phys. Rev. C **89**, 064910 (2014).
[31] C. Gale, S. Jeon, B. Schenke, P. Tribedy, and R. Venugopalan, Phys. Rev. Lett. **110**, 012302 (2013).
[32] M. Floris [Nucl. Phys. A (to be published)] (2014).
[33] V. Begun, W. Florkowski, and M. Rybczynski, Phys. Rev. C **90**, 014906 (2014).
[34] M. Petran, J. Letessier, V. Petracek, and J. Rafelski, Phys. Rev. C **88**, 034907 (2013).
[35] A. Kisiel, T. Taluc, W. Broniowski, and W. Florkowski, Comput. Phys. Commun. **174**, 669 (2006).
[36] M. Chojnacki, A. Kisiel, W. Florkowski, and W. Broniowski, Comput. Phys. Commun. **183**, 746 (2012).
[37] G. Torrieri, S. Steinke, W. Broniowski, W. Florkowski, J. Letessier, and J. Rafelski, Comput. Phys. Commun. **167**, 229 (2005).
[38] J. Letessier and J. Rafelski, Phys. Rev. C **59**, 947 (1999).
[39] J.-P. Blaizot, F. Gelis, J.-F. Liao, L. McLerran, and R. Venugopalan, Nucl. Phys. A **873**, 68 (2012).
[40] J.-P. Blaizot, J. Liao, and L. McLerran, Nucl. Phys. A **920**, 58 (2013).
[41] F. Becattini, M. Bleicher, T. Kollegger, M. Mitrovski, T. Schuster, and R. Stock, Phys. Rev. C **85**, 044921 (2012).
[42] F. Becattini and J. Manninen, J. Phys. G **35**, 104013 (2008).
[43] F. Becattini and J. Manninen, Phys. Lett. B **673**, 19 (2009).
[44] P. Bozek, Acta Phys. Polon. B **36**, 3071 (2005).
[45] S. N. Bose, Z. Phys. **26**, 178 (1924).
[46] A. Einstein, Sitz. Ber. Preuss. Akad. Wiss. (Berlin) **1**, 3 (1925).
[47] J. Zimanyi, G. I. Fai, and B. Jakobsson, Phys. Rev. Lett. **43**, 1705 (1979).
[48] I. N. Mishustin, L. M. Satarov, J. Maruhn, H. Stoecker, and W. Greiner, Phys. Lett. B **276**, 403 (1992).
[49] C. Greiner, C. Gong, and B. Muller, Phys. Lett. B **316**, 226 (1993).
[50] S. Pratt, Phys. Lett. B **301**, 159 (1993).
[51] W. Florkowski and M. Abu-Samreh, Z. Phys. C **70**, 133 (1996).
[52] T. Csorgo and J. Zimanyi, Phys. Rev. Lett. **80**, 916 (1998).
[53] A. Bialas and K. Zalewski, Phys. Lett. B **436**, 153 (1998).
[54] R. Lednicky, V. Lyuboshitz, K. Mikhailov, Y. Sinyukov, A. Stavinsky, and B. Erazmus, Phys. Rev. C **61**, 034901 (2000).
[55] V. V. Begun and M. I. Gorenstein, Phys. Lett. B **653**, 190 (2007).
[56] E. Kokoulina *et al.* (SVD-2 Collaboration), PoS ICHEP **2012**, 259 (2013).
[57] M. H. Anderson, J. R. Ensher, M. R. Matthews, C. E. Wieman, and E. A. Cornell, Science **269**, 198 (1995).
[58] K. B. Davis, M.-O. Mewes, M. R. Andrews, N. J. van Druten, D. S. Durfee, D. M. Kurn, and W. Ketterle, Phys. Rev. Lett. **75**, 3969 (1995).
[59] V. V. Begun and M. I. Gorenstein, Phys. Rev. C **77**, 064903 (2008).
[60] J. Madsen, Phys. Rev. Lett. **69**, 571 (1992).
[61] D. Boyanovsky, H. J. de Vega, and N. G. Sanchez, Phys. Rev. D **77**, 043518 (2008).
[62] T. Kalaydzhyan, Phys. Rev. D **89**, 105012 (2014).
[63] R. Rapp, T. Schäfer, E. V. Shuryak, and M. Velkovsky, Phys. Rev. Lett. **81**, 53 (1998).
[64] K. Splittorff, D. T. Son, and M. A. Stephanov, Phys. Rev. D **64**, 016003 (2001).
[65] B. B. Abelev *et al.* (ALICE Collaboration), Phys. Rev. Lett. **111**, 222301 (2013).
[66] B. B. Abelev *et al.* (ALICE Collaboration), arXiv:1404.0495 [nucl-ex].
[67] B. B. Abelev *et al.* (ALICE Collaboration), Phys. Lett. B **728**, 216 (2014).
[68] M. Petrán, J. Letessier, V. Petracek, and J. Rafelski, J. Phys. Conf. Ser. **509**, 012018 (2014).
[69] I. Melo and B. Tomasik, poster presentation at the *Quark Matter 2014* conference, Darmstadt, Germany, 2014.
[70] D. Prorok, Phys. Rev. C **75**, 014903 (2007).